J. Phys.: Condens. Matter **24** (2012) 226002 (4pp) doi:10.1088/0953-8984/24/22/226002

Magnetodielectric $CuCr_{0.5}V_{0.5}O_2$: an example of a magnetic and dielectric multiglass

Kiran Singh[1], Antoine Maignan[1], Charles Simon[1], Sanjay Kumar[1], Christine Martin[1], Oleg Lebedev[1], Stuart Turner[2] and G Van Tendeloo[2]

[1] Laboratoire CRISMAT, CNRS UMR 6508, ENSICAEN, 6 Boulevard du Maréchal Juin, 14050 Caen Cedex, France
[2] EMAT, University of Antwerp, Groenenborgerlaan 171, B-2020, Antwerp, Belgium

E-mail: charles.simon@ensicaen.fr

Received 19 March 2012
Published 2 May 2012
Online at stacks.iop.org/JPhysCM/24/226002

Abstract
The complex dielectric susceptibility and spin glass properties of polycrystalline $CuCr_{0.5}V_{0.5}O_2$ delafossite have been investigated. Electron diffraction, high resolution electron microscopy and electron energy loss spectroscopy show that the Cr^{3+} and V^{3+} magnetic cations are randomly distributed on the triangular network of CdI_2-type layers. In contrast to $CuCrO_2$, $CuCr_{0.5}V_{0.5}O_2$ exhibits two distinctive (magnetic and electric) glassy states evidenced by memory effects in electric and magnetic susceptibilities. A large magnetodielectric coupling is observed at low temperature.

(Some figures may appear in colour only in the online journal)

In the search for new multiferroic materials, the symmetry of the structure is of prime importance and the possibility offered by magnetic structures to break the inversion symmetry has been used to discover numerous spin induced ferroelectrics and strong magnetoelectric (ME) coupling [1]. In contrast, coupling between a spin glass and ferroelectricity has not been studied so extensively [2, 3]. Cationic disorder induced by substitution on one crystallographic site may generate magnetic and/or electric glassiness depending on the atoms involved. Disorder is in fact well known to be responsible for glassy properties [4–8], as shown in (Sr, Mn)TiO_3 [9, 10].

Recently, polarization and magnetodielectric (MD) coupling in $CuFe_{0.5}V_{0.5}O_2$ spin glass were reported [3]. The vanadium for iron substitution in the $CuFeO_2$ delafossite hinders the long range magnetic ordering at low temperature. $CuCrO_2$ that is an antiferromagnetic compound (T_N = 24 K) spin induced ferroelectric [11–13]; the V^{3+} for Cr^{3+} substitution creates a disorder that favors short range magnetic order, as reported by Nagarajan *et al* [14] and Ataoui *et al* [15, 16], in agreement with pioneer works of Goodenough [17]. The magnetic properties of Cu(Fe, V)O_2 delafossites have already been studied, and we have revisited the properties of $CuCr_{0.5}V_{0.5}O_2$ in the multiglass framework. In the present article, we report magnetic and electric susceptibilities, magnetodielectric coupling and aging effects.

The sample was prepared from a mixture of Cu, Cr_2O_3 and V_2O_5 weighted in the ratio 1:0.25:0.25, pressed in the form of bars, that were put in an evacuated silica ampoule and then heated at 1000 °C. The purity of the sample was checked by x-ray diffraction and the room temperature unit cell parameters, as the $R\bar{3}m$ space group, are in good agreement with the data previously reported [14, 15]. A verification of the crystal structure and the identification of possible ordering induced by the substitution were carried out by transmission electron microscopy (TEM) at room temperature. The electron diffraction (ED) patterns, collected along the major zone axis of $CuCr_{0.5}V_{0.5}O_2$, show sharp spots, evidence of an excellent crystalline quality, and can be unambiguously indexed in the trigonal $R\bar{3}m$ space group. High resolution TEM (HRTEM) was performed to test the sample quality more precisely (i.e. at the local scale), the homogeneity of the cationic composition and also the possibility of local order. A TEM image along the most informative and relevant zone axis is shown in figure 1(a)

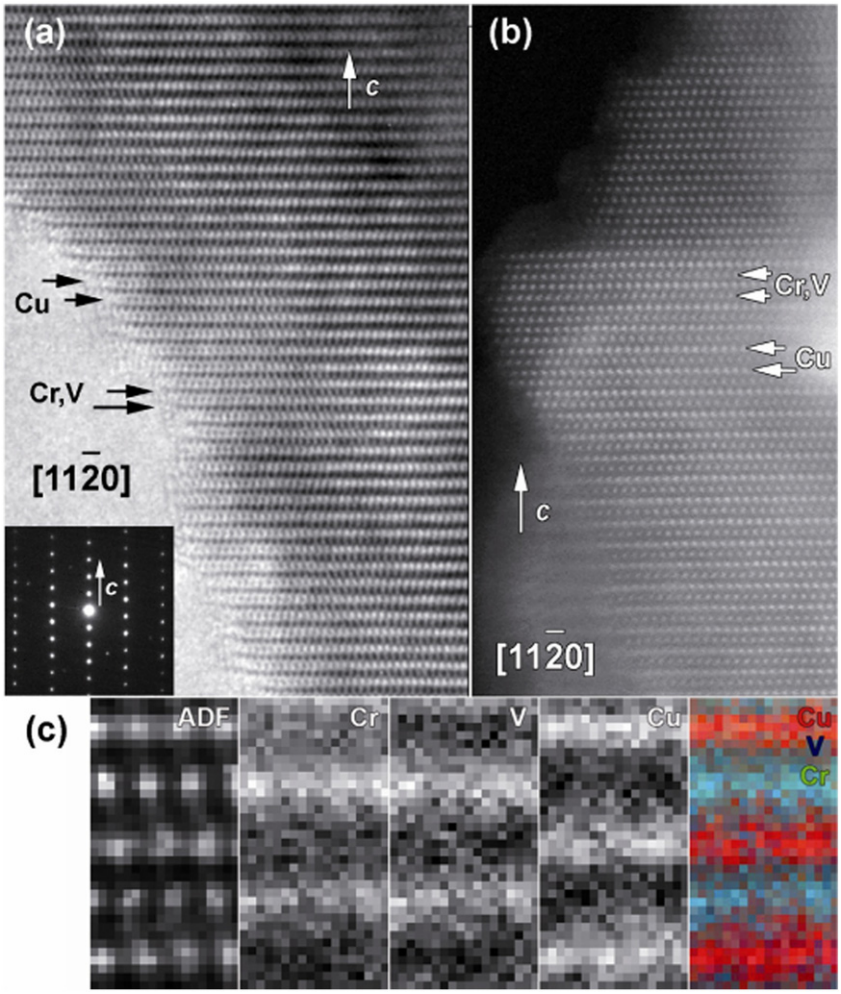

Figure 1. (a) [11$\bar{2}$0] high resolution transmission electron microscopy image of a defect free Cu(Cr–V)O_2 crystal and the corresponding electron diffraction pattern. (b) High angle annular dark field-scanning transmission electron microscopy image along the same zone axis. (c) annular dark field signal and scanning transmission electron microscopy-electron energy loss spectroscopy elemental maps indicating the Cu–Cr/V stacking.

and demonstrates a perfect sequence of alternating Cu and $Cr_{0.5}V_{0.5}$ layers. There is no evidence of segregation or Cr–V ordering either from HRTEM imaging or from ED within a single lamella.

To further investigate a possible ordering of Cr and V, we adopted high resolution (high angle) annular dark field scanning TEM [(HA)ADF-STEM] in combination with spatially resolved electron energy loss spectroscopy (EELS). As HAADF-STEM is a Z-contrast technique (where Z is the atomic number and with so-called mass–thickness sensitivity approximately proportional to Z^2) an ordering of Cr ($Z = 24$) and V ($Z = 23$) might be apparent in high resolution images. In the HAADF-STEM image in figure 1(b) no ordering can be detected; however, one might argue that this is very difficult since Cr and V only differ by $Z = 1$. We therefore acquired atomic resolution EELS data from the region indicated in figure 1(c) (marked ADF) using the spectrum imaging (SI) technique. The acquired EELS data containing the V–$L_{2,3}$, O–K, Cr–$L_{2,3}$ and Cu–$L_{2,3}$ edges were treated by principal component analysis prior to the generation of the elemental maps displayed in figure 1(c). The atomic resolution elemental maps confirm the results from HAADF-STEM and HRTEM—no ordering of Cr or V layers can be detected, not even on a local scale. All layers are homogeneously mixed with Cr and V. A quantification of the composition in the top Cr/V layer yielded 47 ± 5 at.% V and 53 ± 5 at.% Cr, in good agreement with the nominal composition.

The magnetic behavior has been explored by dc and ac magnetic measurements. The dc magnetization was measured in zero field cooled (zfc) and field cooled (fc) modes under different magnetic fields by using a Quantum Design superconducting quantum interference device (SQUID) magnetometer. Isothermal magnetization was also measured at different temperatures, and with a magnetic field up to ±9 T, by using the AC magnetometry system option of a Quantum Design Physical Properties Measurement System (PPMS). The ac magnetic susceptibility (χ) versus temperature was also performed with a PPMS for frequencies ranging from 10 Hz up to 10 kHz. Figure 2 summarizes these data which give evidence of a spin glass phase:

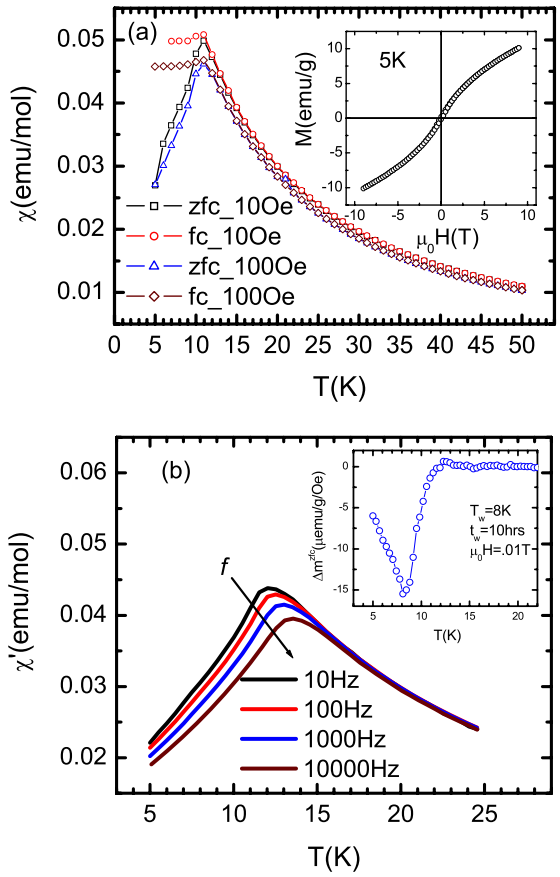

Figure 2. (a) Temperature dependence of the dc magnetic susceptibility in zero field cooled (zfc) and field cooled (fc) mode under two magnetic fields (10 and 100 Oe). The zfc and fc curves are denoted with different symbols. The inset shows isothermal magnetization (at 5 K) as a function of magnetic field. (b) Temperature dependence of the ac magnetic susceptibility at different frequencies. The inset shows Δm^{zfc} versus T measured in $\mu_0 H = 0.1$ T, where Δm^{zfc} is the difference between m^{zfc} with and without an intermediate waiting time t_{w} of 10 h at $T_{\mathrm{w}} = 8$ K.

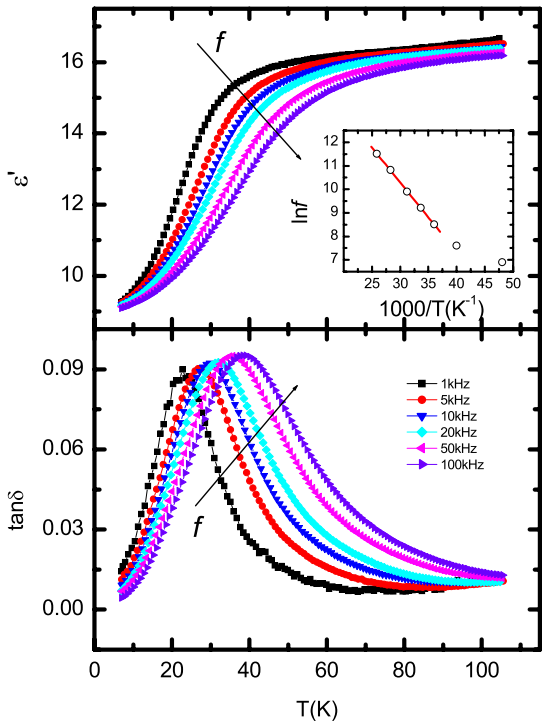

Figure 3. Temperature dependence of the real part and of tan δ (imaginary part) of ac dielectric permittivity at different frequencies (from 1 to 100 kHz) in top and bottom panels, respectively. The inset shows an Arrhenius plot.

(i) a difference between zfc and fc curves, with a field cooled dc magnetization curve which remains temperature independent below the spin glass temperature characterized by a peak in the zfc curve at about 11 K ($=T_{\mathrm{sg}}$) (figure 2(a)),

(ii) a frequency dependence of the maximum of the peak (χ'_{max}) (figure 2(b)),

(iii) and a S-shaped $M(H)$ curve (inset of figure 2(a)).

The frequency dependence of χ'_{max} has been analyzed by a using power law $f \propto f_0 \times (T_{\mathrm{max}}/T_{\mathrm{sg}} - 1)^{z\nu}$. The best fit of the data yields to $f_0^{\mathrm{m}} = 5 \times 10^9$ Hz, $T_{\mathrm{sg}} = 10.6 \pm 0.1$ K and dynamical critical exponent $z\nu = 9$. Memory effect and rejuvenation are also observed below T_{sg} as reported for spin glass [4]. For example, the inset of figure 2(b) reports the magnetization of the sample measured after a waiting time of 10 h at 8 K. This magnetization curve exhibits a clear dip at the corresponding temperature (8 K). All these features are the characteristics of a spin glass phase [5] and strongly suggest that the magnetic structures of $CuCr_{0.5}V_{0.5}O_2$ and $CuCrO_2$ are completely different. Additionally, these results indicate that the dielectric properties of $CuCr_{0.5}V_{0.5}O_2$ should also be different from $CuCrO_2$ in which ferroelectricity is induced by the magnetic ordering. This led us to perform dielectric permittivity measurements.

At low temperature (<250 K) $CuCr_{0.5}V_{0.5}O_2$ is a good insulator with a resistivity larger than 10^6 Ω cm (not shown). This is confirmed by the dielectric permittivity and corresponding losses (tan δ) measured at 1 V ac field amplitude for different frequencies (from 1 to 100 kHz) (figure 3). The real part of the dielectric permittivity is almost temperature and frequency independent between 110 and 80 K. On further cooling, it drops slowly, and clear frequency dispersion can be seen (figure 3(a)) with the imaginary part exhibiting a frequency dependent peak, characteristic of disordered systems (figure 3(b)) [18, 19]. These features are distinct from $CuCrO_2$ for which a clear frequency independent peak is observed at T_{N}. In $CuCr_{0.5}V_{0.5}O_2$, the peak position in tan δ fits with the Arrhenius law at higher frequencies, as for glassy behaviors, and deviates from Arrhenius law at low frequencies (inset of figure 3(a)). The fitted parameters, in the high frequency limit ($f_0^{\mathrm{e}} = 2.14 \times 10^8$ Hz and $E_a = 0.025$ eV or 300 K) are in the range of typical values observed in $(KBr)_{0.50}(KCN)_{0.50}$ (of the order of 10^9) [20], (Sr, Mn)TiO_3 (10^9) [9] or $KTaO_3$ (10^{13}) [21].

To prove the existence of a glassy electric ground state, we have performed aging experiments to test possible memory effects in dielectric susceptibility. Figure 4 shows the difference between curves obtained at 100 kHz, and taken after waiting 5 h at 35 K or 10 h at 25 K. In both cases, a clear

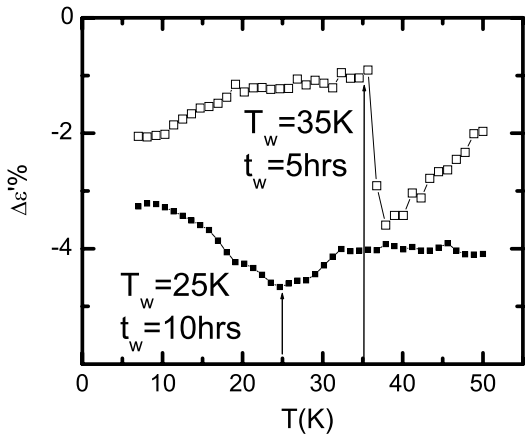

Figure 4. $\Delta\varepsilon'$ (T) curve: aging effect in dielectric susceptibility (at 100 kHz) with T_w and t_w mentioned in the plots {35 K and 5 h} or {25 K and 10 h} and $\Delta\varepsilon' = \varepsilon'_{wait} - \varepsilon'_0$.

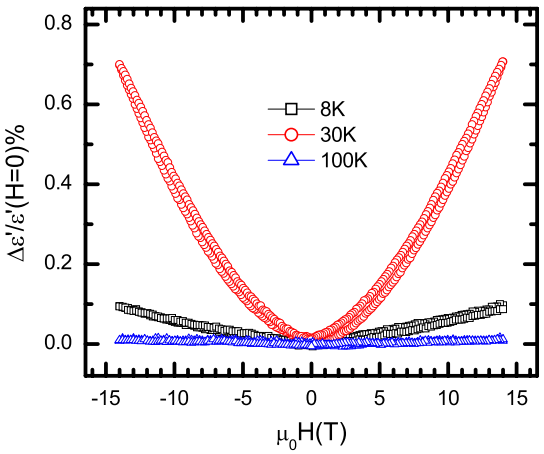

Figure 5. Magnetodielectric coupling at different temperatures.

trough in the dielectric constant curve is observed around T_w, which is characteristic of an electric glassy state [22, 9, 10]. The value $\Delta\varepsilon' = \varepsilon'_w - \varepsilon'_0$ is about -3% at 35 K and 100 kHz, which is similar to Plexiglass (PMMA) but rather small compared to (Sr, Mn)TiO_3. This small value (3%) may indicate that only a small fraction of the system is frozen, but can also be due to a lower relaxation process. No measurable effect was observed above 40 K.

In order to study the interplay between both types of glasses, and following the work of Shvartsman *et al* who measure a linear coupling on $M(E)$ [9], we have measured the magnetodielectric effect $\varepsilon(H)$ in the spin glass phase (8 K) and at higher temperatures (30, 100 K) (figure 5). A large quadratic coupling is observed at 30 K and a smaller one at 8 K, while the effect is much smaller at 100 K. This observation is very different from the situation reported by Shvartsman *et al* who measured a linear effect with a change of sign in M when E changes its sign. This suggests that the microscopic origin of both effects should be different. In particular, the large effect at 30 K (i.e. well above the glass transition) should be related to the existence of very large magnetodielectric effects in the paramagnetic phase as in $Co_3V_2O_8$ [23].

In conclusion, in $CuCr_{0.5}V_{0.5}O_2$, the disorder induced by the cationic substitution leads to spin glass and dipolar glass behaviors, totally different from long range antiferromagnetism and the frequency independent peak in dielectric permittivity reported for $CuCrO_2$. In the spin glass phase, a quadratic magnetodielectric coupling is observed. The existence of two 'glassy order parameters' distinguishes $CuCr_{0.5}V_{0.5}O_2$ from 'classical' multiferroics and rather includes this delafossite in the family of 'multiglass' compounds which is a promising new route for materials which exhibit magnetodielectric coupling.

References

[1] Kimura T, Goto T, Shintani H, Ishizaka K, Arima T and Tokura Y 2003 *Nature* **426** 55
[2] Claridge J B *et al* 2009 *J. Am. Chem. Soc.* **131** 14000
[3] Singh K, Maignan A, Simon C, Hardy V, Pachoud E and Martin C 2011 *J. Phys.: Condens. Matter* **23** 126005
[4] Jonason K, Vincent V, Hammann J, Bouchaud J P and Nordblad P 1998 *Phys. Rev. Lett.* **81** 3243
[5] Mydosh J A 1993 *Spin Glass an Experimental Introduction* (London: Taylor and Francis)
[6] Colla E V, Chao L K, Weissman M B and Viehland D D 2000 *Phys. Rev. Lett.* **85** 3033
[7] Doussineau P, de L, Aroso T and Levelut A 1999 *Europhys. Lett.* **46** 401
[8] Bellon L, Ciliberto S and Laroche C 2000 *Europhys. Lett.* **51** 551
[9] Shvartsmann V V, Bedanta S, Borisov S P, Kleemann W, Tkach A and Vilarinho P M 2008 *Phys. Rev. Lett.* **101** 165704
[10] Kleemann W, Shvartsmann V V, Bedanta S, Borisov P, Tkach A and Vilarinho P M 2008 *J. Phys.: Condens. Matter* **20** 434216
[11] Kimura T, Lashley J C and Ramirez A P 2006 *Phys. Rev.* B **73** 220401(R)
[12] Seki S, Onose Y and Tokura Y 2008 *Phys. Rev. Lett.* **101** 067204
[13] Poienar M, Damay F, Martin C, Hardy V, Maignan A and Andre G 2009 *Phys. Rev.* B **79** 014412
[14] Nagarajan R, Duan N, Jayaraj M K, Li J, Vanaja K A, Yokochi A, Draeseke A, Tate J and Sleight A W 2001 *Int. J. Inorg. Mater.* **3** 265
[15] Ataoui K E, Doumerc J P, Ammar A, Gravereau P, Fournès L, Wattiaux A and Pouchard M 2003 *Solid State Sci.* **5** 1239
[16] Ataoui K E, Doumerc J P, Ammar A, Grenier J C, Fournès L, Wattiaux A and Pouchard M 2005 *Solid State Sci.* **7** 710
[17] Goodenough J B 1976 *Magnetism and the Chemical Bond* (*Interscience Monographs on Chemistry*) vol 1 (New York: Huntington) pp 174–8
[18] Cross L E 1987 *Ferroelectrics* **76** 241
[19] Bokov A A and Ye Z G 2006 *J. Mater. Sci.* **41** 31
[20] Bhattacharya S, Nagel S R, Fleishman L and Susman S 1982 *Phys. Rev. Lett.* **48** 1267
[21] Shvartsman V V, Bedanta S, Borisov P, Kleemann W, Tkach A and Vilarinho M P 2010 *J. Appl. Phys.* **107** 103926
[22] Bharadwaja S S S N, Kim J R, Ogihara H, Cross L E, Trolier-McKinstry S and Randall C A 2011 *Phys. Rev.* B **83** 024106
[23] Bellido N, Martin C, Simon C and Maignan A 2007 *J. Phys.: Condens. Matter* **19** 056001